Analytical capabilities of the V.G. Khlopin Radium Institute in view of nuclear forensics challenges

Y. Panteleev

V.G. Khlopin Radium Institute
St Petersburg, Russian Federation

Abstract. The V. G. Khlopin Radium Institute is Russia's leading organization providing technical services in radiochemistry to the nuclear industry. Its activities include research and development, analytical laboratory services, environmental investigations, waste treatment engineering, accident response, and production of specialized nuclear materials such as radioisotopes, isotopic standards, labeled organic compounds, sources, and radiation detectors. The Radium Institute has, since its establishment in 1922, maintained the highest scientific standards. In 1974 the Institute joined IAEA Network of Analytical Laboratories (NWAL) and as such is qualified currently for analysis of nuclear material and environmental samples, provision of reference materials and quality control (QC) functions.

1. Introduction

The main tasks in the industry
- Development and application of high-sensitive and precision methods of NM analysis
- Analysis of NM in any matrices and in all ranges of concentrations:
- Determination of radionuclide composition of SNF
- Determination of burnup of high- burn-up fuel
- NM isotopic composition and content in the environmental samples and RAW
- Manufacturing of and supply to the industry enterprises of the NM reference materials

The tasks of the KRI in cooperation with the IAEA
- Analysis of the inspectorate samples for IAEA safeguards
- Development of high-sensitive and precision analytical methods for NM measurements
- Development of and participation in the Quality Assurance Programs for analytical measurements
- Manufacturing of and delivery to the IAEA NM Reference materials

Analytical methods of NM measurements
- Isotope dilution mass-spectrometry
- Precision spectro-photometry
- Titrimetric methods
- Luminescence of uranium and neptunium
- Chemical-spectral trace analysis
- The alpha, beta, gamma radiometry
- Neutron analytical methods

Y. Panteleev

Table 1. Measurement parameters

Method	Uncertainty	Detection limit
Laser-luminescent of uranium	5-10 %	in solutions - 10^{-11} g/ml; in soil and plant ash – 0,01 ppm
Laser-luminescent of plutonium	5-10 %	in solutions– $5 \cdot 10^{-11}$ g/ml; in soil and plant ash – 0,05 ppm
Isotope dilution mass-spectrometry of uranium, plutonium, americium, curium	≤ 0,1÷0,2 %	^{238}U – 10^{-12} g Other isotopes – 10^{-14} g plutonium – 10^{-15} g americium – 10^{-15} g
Isotope dilution alpha-spectrometry of plutonium	≤ 0,5÷0,6 %	10^{-12} g
Potentiometric determination of uranium	≤ 0,1 %	10 mg
Spectro-photometric determination of uranium and plutonium by self-absorption	≤ 0,1÷0,2 %	100 mg
Spectro-photometric determination of uranium and plutonium and thorium with arsenazo III	≤ 0,1%	10 mkg
NM gamma-spectrometric determination	≤ 5 %	uranium ~ 50 mkg plutonium ~ 50 ng
Alpha-spectrometric determination of plutonium, uranium, neptunium, americium	5-8 %	$5 \cdot 10^{-4}$ Bq/g

2. Conclusion

The combination of the methods available at the KRI and the experience gained in analytical research and development makes it possible to be confident in getting analytical signatures of the investigated nuclear materials in view of nuclear forensics challenges.

i2®©: Investigative and Interpretive Radiochemistry - The Precursor to Nuclear Forensics

P. Thompson[†]

AWE
Aldermaston, Reading, Berkshire
RG7 4 PR
United Kingdom

Abstract. In the early 1990's when radioactive material began to feature in legal proceedings following its interception by Government Agencies there was a requirement for analysis of the material to support the judicial process. This requirement went on to grow into what is now commonly known as Nuclear Forensic Science.

Since the discovery of radioactivity at the close of the 19th Century the science of radiochemistry has developed to address topics related to the uses of radioactivity. The techniques developed over the roughly 100 years between the discovery of radiochemistry and the early 1990s form the basis of Nuclear Forensic Science. This paper will highlight some of the achievements of the radiochemistry community in the century prior to 1990 which were available to be used and built upon as validated science to support the needs of the legal and judicial communities when required in the last two decades as part of the Nuclear Forensic Science Community.

1. Introduction

In the early 1990's when radioactive material began to feature in legal proceedings following its interception by Government Agencies there was a requirement for analysis of the material to support the judicial process.

This requirement went on to grow into what is now known as Nuclear Forensic Science. The claims made for Nuclear Forensic Science are many and varied, but can be reduced to answering the following questions – the 'W' questions:

- what is the material,
- who has handled the material,
- where has it been,
- where did it come from,
- what was its intended use,
- when was it made,
- who lost it.

At first sight answering these questions from the analysis of a small portion of confiscated material might appear to be verging on the impossible. However it continues to be shown that radiochemical techniques, alongside other scientific practices, can if not exactly answer the questions at least rule options out and point in general directions.

[†] E-mail address of corresponding author: Paul.Thompson@awe.co.uk

A lot of the basic science behind Nuclear Forensic Science is formed around the science of Radiochemistry. Since the discovery of radioactivity at the close of the 19th Century the science of radiochemistry developed to address many topics related to the uses of radioactivity. The techniques developed over the roughly 100 years between the discovery of radiochemistry and the early 1990s form the basis of Nuclear Forensic Science. To modernise nomenclature I have rebranded radiochemistry as **i²®©** - investigative and interpretive radiochemistry.

This paper will highlight some of the achievements of the radiochemistry community in the century prior to 1990. It is the techniques developed in this time that were available to be used and built upon as validated science to support the needs of the legal and judicial communities as part of the Nuclear Forensic Science mission.

2.   The Discovery of Radioactivity and the Development of Radiochemistry.

The discovery of radioactivity was accidental. In 1898 Henri Becquerel was forced to postpone his experimental programme, studying uranium fluorescence caused by sunlight, due to a period of cloudy weather. He put the uranium mineral in a drawer with the photographic plate. When he developed the plate he was surprised to see the image as bright as when the experiment was conducted in full sunlight.

The Curies, Marie and Pierre, began investigating uranium minerals. During these investigations they isolated two new elements – polonium and radium, which were 60 and 400 times more radioactive than uranium. The starting material was 2 tonnes of the uranium mineral pitchblende, and by the use of successive precipitation and crystallisation stages they produced about 0.1g of pure radium, about 2,600 MBq. The Curies, with Henri Becquerel, were awarded the 1903 Nobel Prize for Physics.

In his Acceptance speech on 6th June 2005 in Stockholm Pierre Curie finished the speech with the following:

"….It can even be thought that radium could become very dangerous in criminal hands, and here the question can be raised whether mankind benefits from knowing the secrets of Nature, whether it is ready to profit from it or whether this knowledge will not be harmful for it. The example of the discoveries of Nobel is characteristic, as powerful explosives have enabled man to do wonderful work. They are also a terrible means of destruction in the hands of great criminals who are leading the peoples towards war. I am one of those who believe with Nobel that mankind will derive more good than harm from the new discoveries".

This can be interpreted as the first call to develop Nuclear Forensic Science – Pierre Curie was warning of the dangers of Criminals possessing radioactive materials; designation as a crime requires laws to be passed for prosecution; prosecution requires the presentation of evidence and this leads to the need for Nuclear Forensic Science – it took around 90 years for the criminal and judicial / legal communities to catch up!

Elsewhere in the speech Pierre points out that there are many scientists, alongside his wife and himself who are investigating radioactivity - Rutherford, Debierne, Elster and Geitel, Giesel, Kauffmann, Crookes, Ramsay, Soddy, Meyer and Schweidler, Becquerel, Mme. Curie, and Villard; that three different emissions had been identified – α -, β – and γ – rays. He stated that radioactivity had only been found associated with uranium and thorium; that actinium had been discovered; that methods of radiation detection had been invented - discharge of an electroscope by the rays from the induced radioactivity, phosphorescence of zinc sulphide under the action of the emanation – later shown to be alpha particles from Rn-222 .

The subsequent discovery of the neutron, understanding of isotopes, and development of the Geiger Counter and Mass Spectrometer were the results of a large body of research and development. By the late 1930's this led to the discovery of man made radioactivity, neutron fission of uranium, and the discovery of neptunium and plutonium.

There were many new additions to the list of scientists involved: Lawrence, Chadwick, Cockroft, Walton, Szilard, Fermi, Hahn, Strassmann, Meitner, Frisch and Seaborg. As with the previous list, it includes both chemists and physicists – radiochemistry being a subject that require skills from both disciplines working in partnership.

3. The Development of the Nuclear Industry

The Second World War led to the foundation of a nuclear industry, initially to support the production of the atom bomb, and then post war a civil nuclear industry. Radiochemistry had a large part to play in the development of the nuclear fuel cycle

Firstly, laboratory radiochemistry at the atom to milligram scale had to be translated into a production capability dealing with kilograms of material, especially for the recovery of plutonium, where it was kilograms of plutonium from tonnes of highly radioactive irradiated uranium, this meant the production radiochemistry had to be conducted remotely behind radiation shielding.

Secondly there was a need for quality control / assurance on the product – this required the analysis methods being developed to be validated to ensure the product was fit for purpose; this requirement being for both civil and military production schemes. It is these methods, with further developments since, that form the basis of fingerprinting the manufacturing processes that feed into answering some of the 'W' questions at the start of this paper.

The initial production processes were scaled up versions of the laboratory radiochemistry analysis methods. Over time improvements and changes were made to the processes, both to improve the quality of the product, and the efficiency of the processes. There were many different processes and capabilities trialled and developed by different countries and industrial companies, and to some extent this work is continuing to this day – studies to make the fuel cycle proliferation resistant. The legacy data from these 'development processes' feed into answering the 'W' questions.

Having created an industry it was necessary to regulate it, not only from the Health and Safety aspects, but also for the nuclear proliferation aspects – preventing the spread of nuclear weapons. Starting in the 1950's with the creation of the IAEA, and in Europe Euratom, bodies were set up to 'regulate' the nuclear industries. To encourage nations to work together there were a number of treaties agreed that put the regulation into effect, e.g. various Test Ban Treaties, culminating in the Comprehensive Test Ban Treaty, and the Non-Proliferation Treaty with updates. These organisations and treaties have led to the development of capabilities to carry out surveillance that the Treaties are being observed, and these techniques are available to help answer the 'W' questions.

4. Radiochemistry Outside the Nuclear Industry

The last few paragraphs have dealt with the application of radiochemistry to the development of the nuclear fuel cycle. There have been other areas that radiochemistry has been applied to: health and safety, environmental surveillance, medicine, geochemistry, and archaeology. Techniques from all of these areas are available to answer the 'W' questions. For example geochemistry makes much use of isotope ratio measurements, both to fingerprint the origins of material, e.g. oxygen isotope ratios, lead isotope ratios, and to age date events in geological time. Archaeology uses C-14 dating to date biological materials. Specific cases of these techniques being used for the 'W' questions are the determination of the ratios of the lanthanide elements to each other in uranium ores and concentrates, and age dating of uranium and plutonium materials based on the amounts of daughter radionuclides that have grown in since their last processing.

5. Future Developments

The impression could be gained from the preceding that everything was covered and was in place to fully support Nuclear Forensic Science in the 1990's, however, some deficiencies did exist, and there

are always methods that can be improved, new equipment that can be applied and limits of detection that can be reduced.

The main deficiencies identified were that because the measurements in the past were not carried out for Nuclear Forensic Science purposes, they did not record all the data that a modern Nuclear Forensic investigation would generate. For example samples of uranium oxide analysed in the 1950's, prior to use as fuel in a nuclear reactor, did not have a full elemental fingerprint recorded for a combination of reasons – it was not necessary, and the contemporary equipment could not measure to the low limits of today's instrumentation. This means that care has to be taken when comparing new analysis data with old records – both as regards to if the element was measured, and the accuracy and precision of the different data sets by different methods.

A major area for development that has been highlighted is the need for Standard Reference Materials. These are necessary for method validation to ensure that any data presented in Court can be shown to have come from a fully validated method, carried out by trained staff on a calibrated instrument.

ACKNOWLEDGEMENTS

Capabilities of Hybrid SIMS-SSAMS System for Nuclear Forensics Applications

K.S. Grabowski, K.C. Fazel, D.L. Knies[1]

Naval Research Laboratory
Materials Science and Technology Division
Washington, DC 20375
United States of America

Abstract. Mass spectrometry of particulate samples by Secondary Ion Mass Spectrometry (SIMS) is a very useful nuclear forensics tool. However, there are limitations caused by interferences from molecular species, such as $^{238}U^1H$ while measuring ^{239}Pu. These interferences ($> 10^4$ M/ΔM) can exceed the resolving power of SIMS. Accelerator Mass Spectrometry (AMS) is capable of eliminating such molecular ion interferences, but lacks spatial information and generally requires use of negative ions. This requirement limits its sensitivity, since actinide and lanthanide elements preferentially generate positive atomic ions ($\sim 10^4$: 1). The US Naval Research Laboratory (NRL) has installed a hybrid SIMS-AMS system, using a Single Stage AMS (SSAMS) as a replacement for the normal Cameca IMS 4f SIMS electron multiplier detector. The NRL design enables analysis of either positive or negative ions. Thus, this system offers the potential to provide SIMS-like particle analysis without the forest of signals from molecular species, and is capable of measuring important positive atomic ions. This should improve measurement sensitivity and precision to determine isotopic distributions of actinides, lanthanides, and transition metals; and elemental abundances of trace species in particles or small features. Initial measurements and instrument capabilities are described.

1. Introduction

Secondary Ion Mass Spectrometry (SIMS) is a well-developed microanalysis tool, and is employed for particulate analysis in nuclear forensic examinations. However, interferences from molecular species with nominally the same mass as an isotope of interest cause sensitivity limitations. For masses beyond 90 u, the resolution required to reject interferences can exceed 10^4 M/ΔM, which is a challenge for SIMS. Examples of the resolution required at a given isotopic mass to reject binary molecules containing H, C, or O are shown in Fig. 1. Ternary molecules can create even greater challenges.

On the other hand, Accelerator Mass Spectrometry (AMS) is a well-developed tool for precise isotopic analysis of bulk material. By accelerating analyzed ions to high energy, they can transit a gas cell to destroy all molecules, thereby removing interferences. In the case of ^{14}C, residual molecules of ^{13}C-H and ^{12}C-H_2 can be rejected to levels below 10^{-15} of the ^{12}C intensity. However, conventional AMS instruments employ negative ions for analysis; so suffer from diminished sensitivity for electropositive species, such as actinides, lanthanides, many transition metals, and alkali and alkali-earth elements. While molecular ions, such as oxides, are used to improve sensitivity, this approach adds complexity to the analysis and cannot always be used. Additionally, AMS is a bulk analysis technique; so individual particles are not measureable.

---

[1] Present address: Coolescence Inc., Boulder, CO 80301, United States of America
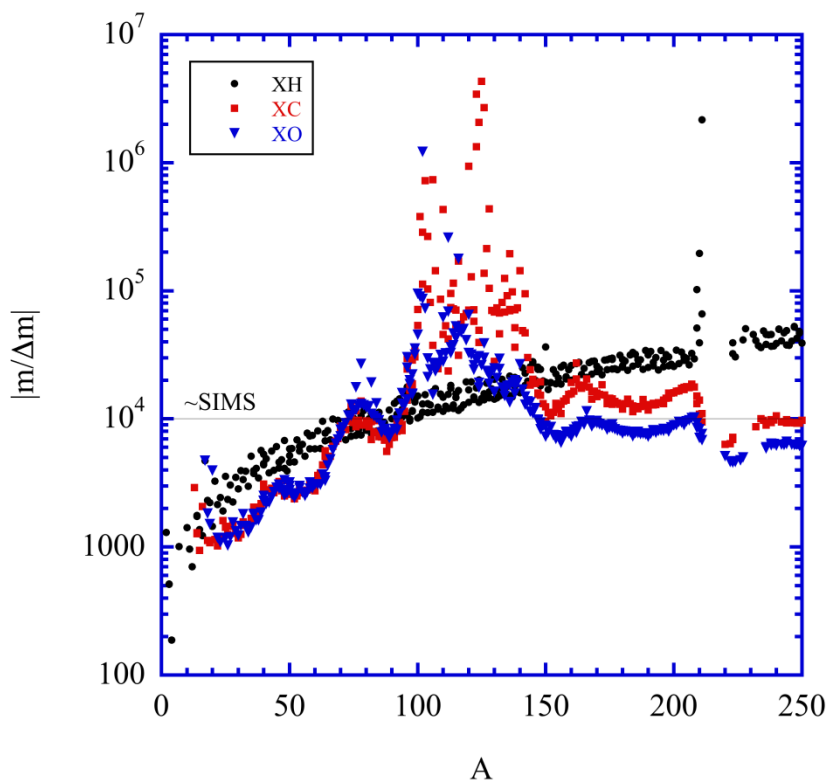
FIG. 1. Mass resolution needed to separate atomic species of interest from binary molecules containing H, C, or O. Above atomic mass of 90, SIMS is strongly challenged by these molecules. This includes the second and third row transition metals, lanthanides, and actinides.

While a SIMS instrument has been combined with a conventional AMS previously [1, 2, 3, 4, 5], these devices were only able to measure negative ions from the SIMS. With recent developments in AMS technology, specifically, Single Stage AMS (SSAMS) instruments [6], it is now possible to perform AMS on positive ions as well [7]. This offers an opportunity to build a cornerstone instrument, combining the advantages of SIMS and AMS for particulate analysis of electropositive elements. As illustrated in Fig. 2, bulk measurements with few molecular ions is provided by Inductively Coupled Plasma Mass Spectrometry (ICPMS) for positive ions, and free of molecular ions by AMS for negative ions. SIMS generates either positive or negative ions and provides spatial resolution, but suffers from molecule interferences. By using a SIMS instrument to generate desired positive (or negative) ions from particulates, and a bipolar SSAMS instrument to destroy molecular ions and measure the residual atomic isotopes, one can construct such a cornerstone instrument (see dark grey blocks in Fig. 2); and that is what the Naval Research Laboratory (NRL) has done.

2. Atomic ion SIMS (ai-SIMS) instrument at NRL

The ai-SIMS instrument at NRL is comprised of a Cameca IMS 4f SIMS instrument generating 4.5 keV positive ions, but where the conventional electron multiplier detector has been replaced by a larger than normal National Electrostatics Corp. SSAMS system operating at up to ±300 kV. It is larger to accommodate a magnet to analyze 75 MeV·u ions, or 246 u ions @ 300 kV. The two systems are joined by an Einzel lens and steering elements. The main elements of the SSAMS system are shown in Fig. 3.
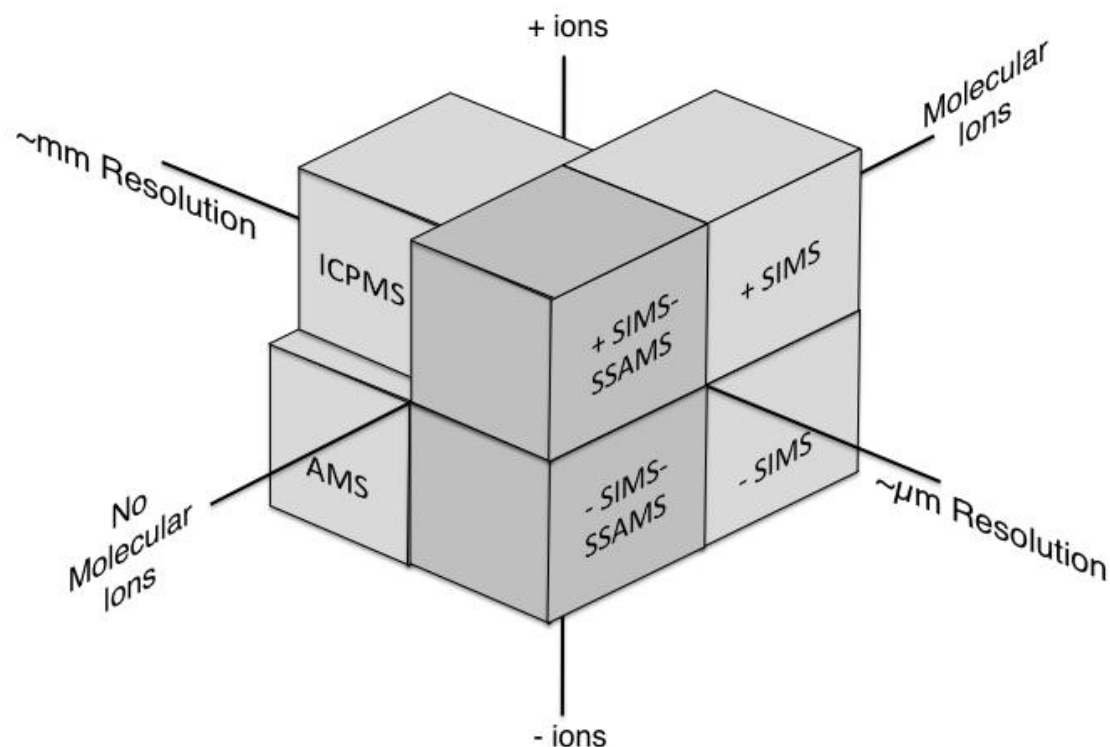
FIG. 2. *Attributes of different mass spectrometric techniques: ICPMS, AMS, SIMS, and hybrid SIMS/SSAMS. The preferred quadrant for actinides, lanthanides, and other electropositive elements in particulate samples is the corner occupied by the hybrid technique.*

They include an injection magnet, acceleration tube, molecule destruction chamber, analyzing magnet, electrostatic analyzer, and electron multiplier detector. Power to operate components on the high voltage deck is provided by a pair of motor-generator sets, although only one set is depicted in Fig. 3.

Because both magnets in the SSAMS system are large, the response time to change the field is long. To expedite switching between masses, the SSAMS is provided with beam-energy "bouncing" through both magnets. This alters the ion beam energy for its transit through a magnet, so the mass-energy product required by the magnetic field can remain constant, but a different mass can be selected. For the analyzing magnet, the energy can be bounced $\pm$ 20 keV, or $\pm6.5\%$ at 304.5 keV, meaning the mass can be bounced $\pm6.5\%$ at 304.5 keV. Larger changes require either lowering the accelerating voltage so the bouncing voltage is a larger percentage, or changing the magnetic field. For isotopic distributions or nearby elements, this would not be necessary.

From previous efforts at NRL to combine SIMS with a tandem accelerator for trace element analysis [8], we learned that charge state (q) +1 ions are preferred for this type of analysis. At a higher q, molecule fragments can create ambiguities with atomic ions. These occur when a fragment's fraction of the original molecule mass (equal to the mass under examination) is nominally equal to the ratio of its q to that of the atomic species investigated. For example, if ^{236}U is selected for analysis at a q of +2 at energy E, then a molecule of $^{118}Sn_2$ at energy E could fragment and produce a $^{118}Sn^{+1}$ ion, at an energy of 0.5 E, since the two molecule fragments equally share the initial energy. Since electrostatic analysis selects ions based on E/q, it would not differentiate between $^{236}U^{+2}$ and $^{118}Sn^{+1}$-fragment ions.
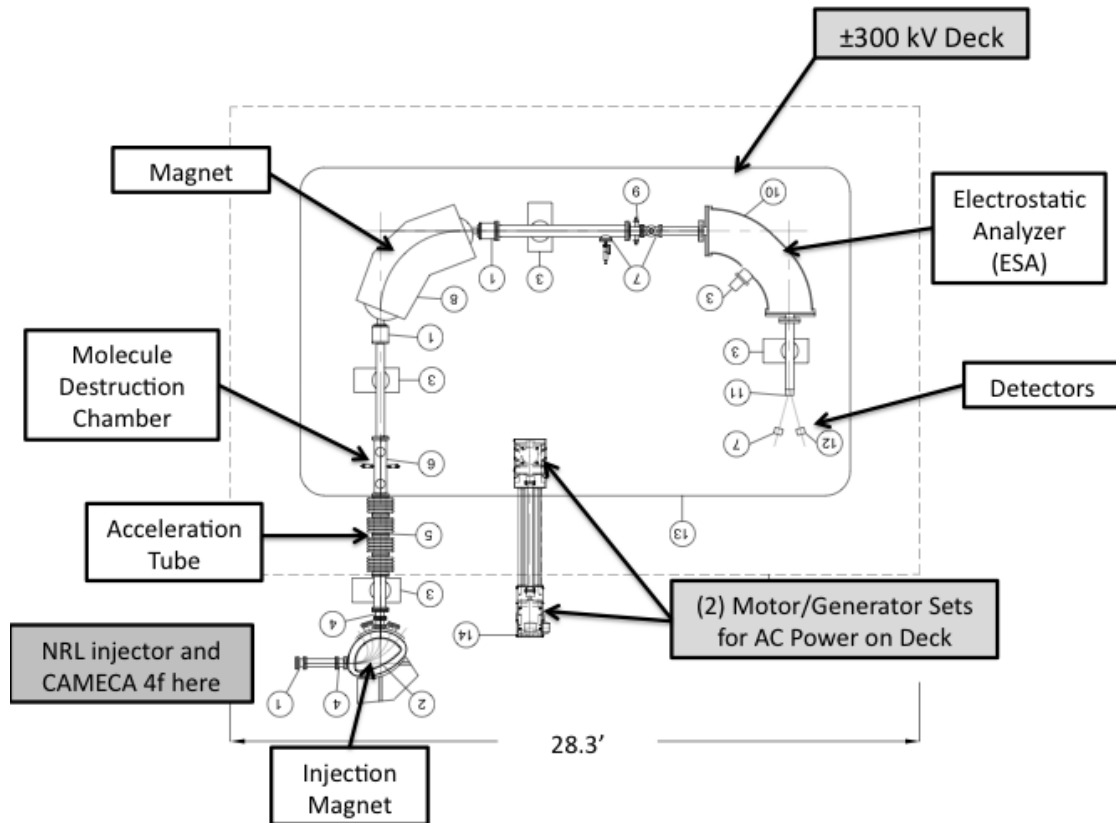
FIG. 3. SSAMS components shown are coupled to Cameca IMS 4f output to replace its normal electron multiplier. Connecting components include an electrostatic lens and steering element to optically match the two instruments. The SSAMS system accelerates ions 300 keV to enable molecule destruction in a gas cell, then performs mass spectrometry. Energy bouncing with a constant magnetic field enables fast switching of nearby masses (±6.5%)

Similarly, since a magnet selects ions based on $(M/q) \cdot (E/q)$, where M is atomic mass, it would not discriminate between these two ions either. By choosing to analyze +1 ions, since this is the lowest q possible for analysis, no molecule fragments exist in a lower charge state to generate an ambiguity.

While SSAMS has been well tested and qualified for its primary application of radiocarbon analysis, there has been little work to date for applications at higher masses. Nevertheless, there is sufficient data to suggest viability of the concept for nuclear forensics applications. To fully implement this concept, some baseline performance characteristics need to be determined. These include a determination of the gas pressure required (for each gas, ion, and energy used) to obtain an equilibrium charge state distribution, and identification of the optimal gas and ion energy to produce the largest fraction of charge state 1+ ions. Vockenhuber et al. [9] showed (see Fig. 4) that while He gas is well suited for producing U^{+2} ions at energies down to 80 keV, other gases such as Ar, Kr and H might be better suited for producing U^{+1} ions. These gases and perhaps others will need to be evaluated for the best production of +1 ions. Additional factors that need to be ascertained are the ability of various gases to sufficiently destroy molecules at different ion energies; the magnitude of atomic beam attenuation that occurs at each of those conditions; and the stability, precision, and detection efficiency obtainable from the instrument.
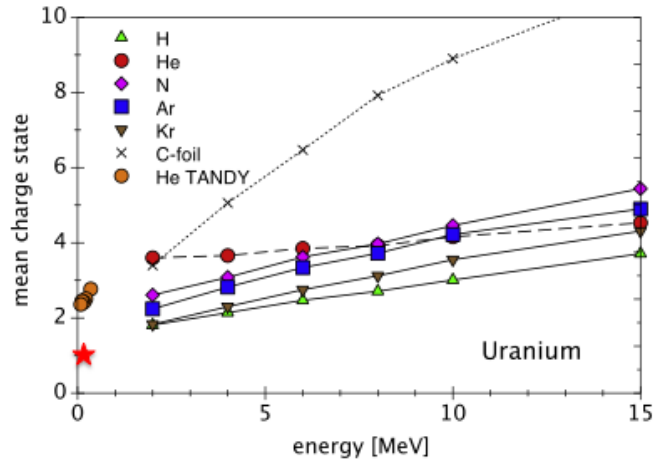
FIG. 4. *While Fig. 1 from Volkenhuber et al. [9] shows He gas is well suited for producing U^{+2} ions at low energies, the trend with energy suggests other gases such as H, Ar, or Kr may be better suited for producing U^{+1} ions at low energy, approaching the location of the star (reprinted with permission from Elsevier).*

3.   Initial measurements

While only enabled for preliminary measurements in April 2014, the NRL ai-SIMS facility has already demonstrated viability of the proposed concept. Preliminary data was collected from samples of Ti, In, Cu, and HfH_2 for atomic and molecular positive ions while operating at 300 kV, using Ar gas for molecule destruction.

3.1.   *Molecule breakup*

The selected samples were used to produce abundant +1 ions of TiO, InO, Cu_2, and HfH. The intensity of each was measured as the pressure of Ar was incrementally changed. As expected, the intensity diminished exponentially with increasing Ar pressure. Data for the $^{63}Cu_2$ molecule is shown in Fig. 5. In this case, the decay is diminished at low intensities, as would be the case if an impurity of ~ 10 ppm of ^{126}Te was present in the Cu sample. Note that over the range of Ar pressures applied, the molecule intensity decreased by over seven orders of magnitude.

3.2.   *Atomic ion attenuation*

Atomic +1 ions of Ti, In, Cu, and Hf were measured to evaluate attenuation of their intensity caused by the use of Ar gas. Data for the attenuation of ^{63}Cu is shown in Fig. 6. Again the expected exponential decay is observed, but in this case, a reduction of only 70% is observed upon using the same highest pressure as used for the $^{63}Cu_2$ breakup measurement.

3.3.   *Cross sections*

The observed exponential decay in intensity is related to the cross section for an Ar atom to either destroy the incident molecule; or to scatter the incident atomic ion out of the required trajectory to be measured. The decrease in ion intensity with increasing gas thickness is described by
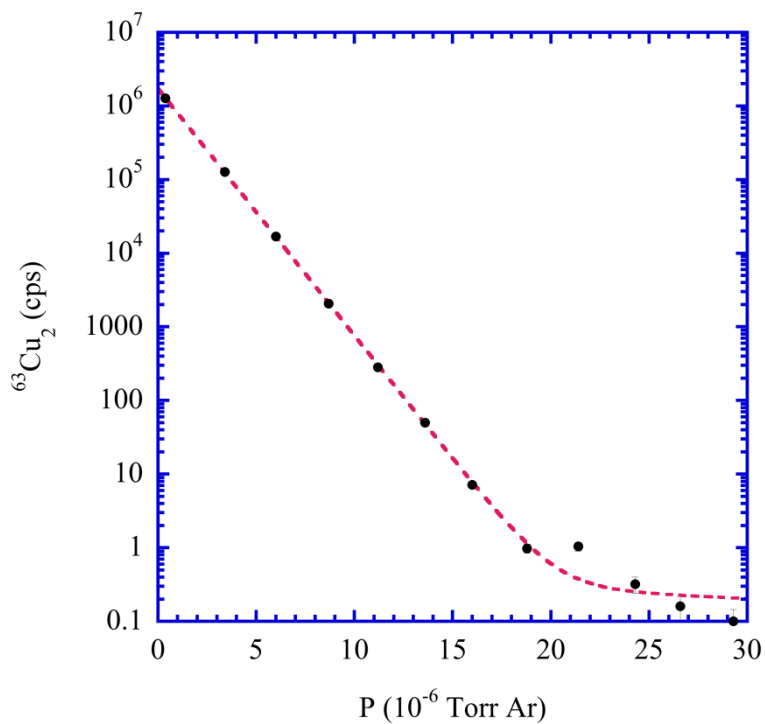
FIG. 5. Intensity decrease of $^{63}Cu_2$ molecule with increasing Ar gas pressure. Two exponentially decaying terms were fit to the data, with the slower decay consistent with a presence of ~10 ppm ^{126}Te.
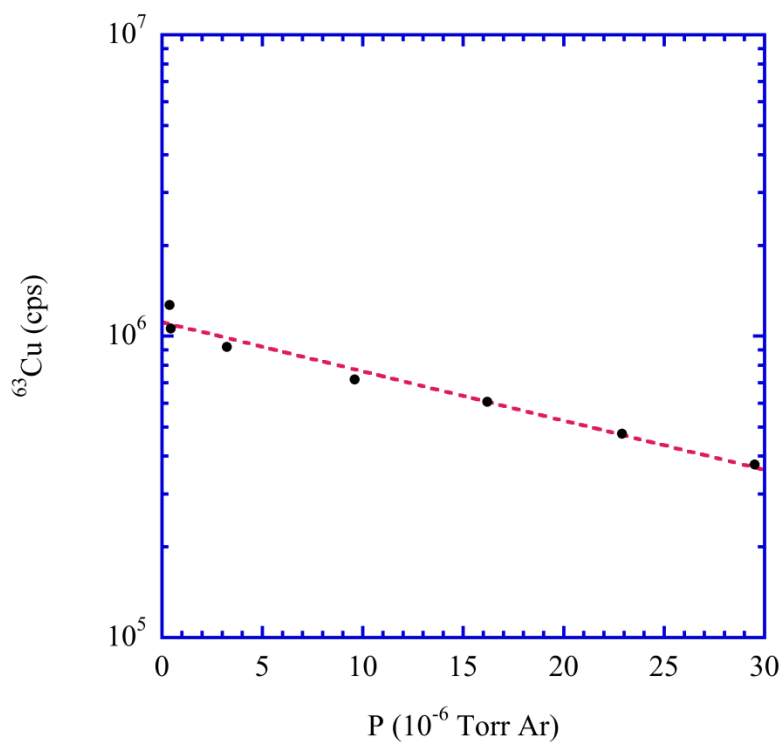

FIG. 6. Intensity decrease of ^{63}Cu atomic ion with increasing Ar gas pressure.

6

$$I = I_0 \exp(-\sigma \cdot N_{Ar} \cdot x_{Ar}) \qquad (1)$$

where

I   is intensity measured with Ar present
I_0 is intensity measured with no Ar present
σ is cross section per Ar atom (cm^2)
N_{Ar} is density of Ar gas (cm^{-3})
x_{Ar} is path length through Ar gas (cm)

The Ar density can be determined from its pressure and temperature through the ideal gas law, so the pressure reported in the data collected can be used along with the path length of the ions through the molecule destruction chamber to convert slopes on semi-logarithmic plots into the cross sections of interest. In this preliminary work, the Ar pressures were measured outside of the actual molecule destruction chamber, but were converted into an average pressure inside the chamber based on information provided by the SSAMS manufacturer.

Molecule destruction cross sections for the various ions measured is shown in Fig. 7a, while those for attenuation of atomic ions is shown in Fig. 7b. In both cases cross sections are similar amongst measured ions, despite differences in molecule type and binding energy, and in ion mass. This suggests a common mode of operation is feasible. Strikingly, there is a ~20 fold difference in cross section between molecule destruction and atomic ion attenuation. This result provides strong evidence the concept behind ai-SIMS is a valid and useful method.
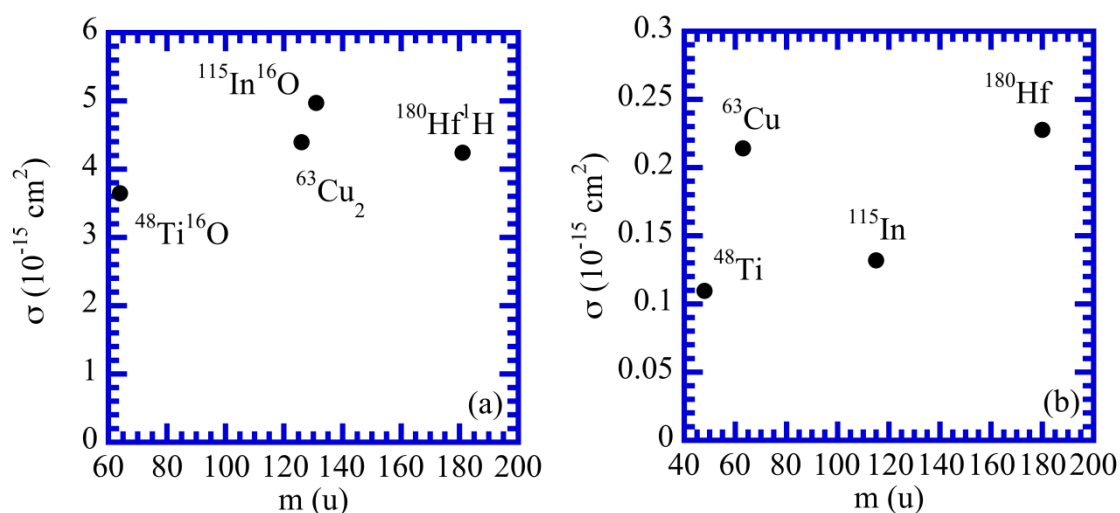
FIG. 7. *Cross sections computed for a) molecule breakup of TiO, InO, Cu_2, and HfH, and b) attenuation of atomic ions of Ti, In, Cu, and Hf, with use of Ar gas and 300 keV ions. Note the factor of ~20 difference between molecule breakup and atomic attenuation values, and the commonality of values amongst the different masses and molecule types.*

3.4. Hydride interference for Hf isotopes

To demonstrate the relevance of ai-SIMS to nuclear forensics issues, Fig. 8 shows the effect of hydride molecules on the apparent isotopic distribution of Hf. As a greater amount of Ar gas is employed, the measured distribution more closely approaches that of the natural abundances expected. As this is preliminary data, the agreement is not exact, but the trend is clear. While this seems like an extreme example, since the sample was HfH_2, it demonstrates a real problem if one wants to measure a small amount of ^{239}Pu while a larger quantity of ^{238}U is present, and hydrides are able to form.
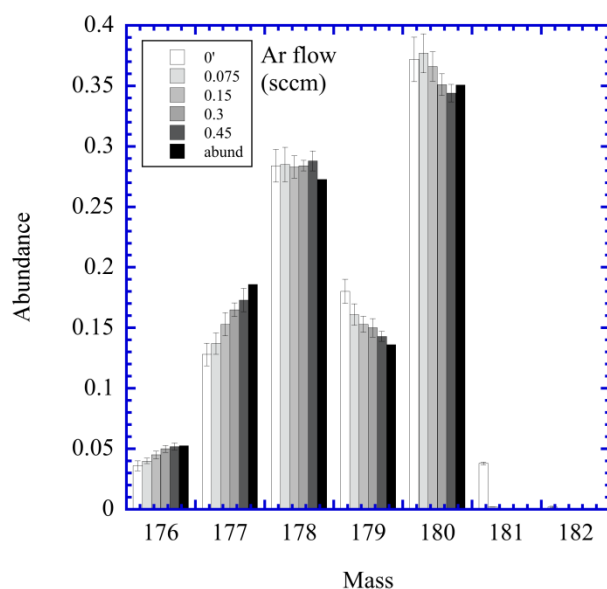
FIG. 8. *Hydride molecules impact the apparent isotope distribution of Hf, when a HfH$_2$ compound is measured. The natural abundance is shown as black bar; with measured intensities approaching the natural abundance as Ar gas flow and molecule destruction increases. The data was normalized by summing the isotope contributions to 1.*

4. Importance to nuclear forensics

Mono-hydride rejection by SIMS requires a mass resolution near 40,000 to measure isotopes of importance to nuclear forensics. With interfering molecules in parentheses, some isotopes of interest include ^{236}U (^{235}U·H) and ^{239}Pu (^{238}U·H) that reveal exposure to neutrons; ^{231}Pa (^{230}Th·H) and ^{210}Pb (^{209}Bi·H) that are indicators of age since chemical separation; ^{233}Pa/^{233}U (both ^{232}Th·H) that can indicate repurposing of ^{232}Th; ^{206}Pb (^{205}Tl·H) as a collateral fingerprint; and ^{210}Po (^{209}Bi·H) and ^{240}Pu (^{239}Pu·H) that can be a weapon component. By eliminating hydride molecules, ai-SIMS could provide greater precision and accuracy to measure these isotopes. Even for small particles where too few atoms of a trace isotope are expected to be observable, evidence of "spoofing" could be obtained due to non-uniformity in concentration leading to some particles having above average concentration that could be measured.

Besides the above-mentioned examples, greater sensitivity for trace elements and isotopic distributions may provide additional fingerprints for source material identification. Rare earth elements and transition metals are such candidates, as they are subject to molecule interferences that challenge the ability of SIMS alone to provide an assay of their content. The use of ai-SIMS may offer access to improved fingerprinting capabilities.

The existing ai-SIMS instrument at NRL is a prototype, hopefully able to contribute to important measurements, but also is intended to evaluate the performance characteristics of ai-SIMS and explore possible refinements to enhance its capabilities. For example, if the ion energy can be reduced, the SSAMS size could be reduced by a commensurate amount, potentially making the concept more widely available.

5. Conclusions

A novel concept known as atomic ion SIMS, or ai-SIMS, is under development at the Naval Research Laboratory to improve sensitivity and precision for microanalysis of particulates of interest to the nuclear forensics community. This approach will greatly reduce molecular ion intensities, so that trace quantities of isotopes and elements can be better quantified. Preliminary data has demonstrated that the concept is valid, and efforts to bring the hybrid instrument to full operation are underway.

REFERENCES

[1] FREEMAN, S.P.H.T., RAMSEY, C.B., HEDGES, R.E.M., "Imaging AMS", Nucl. Instrum. Meth. B 92 (1994) 231.

[2] ENDER, R.M., DOEBELI, M., SUTER, M., SYNAL, H.-A., "Accelerator SIMS at PSI/ETH Zurich", Nucl. Instrum. Meth. B 123 (1997) 575.

[3] DATAR, S.A., RENFROW, S.N., GUO, B.N., ANTHONY, J.M., ZHAO, Z.Y., MCDANIEL, F.D., "TEAMS Depth Profiles in Semiconductors", Nucl. Instrum. Meth. B 123 (1997) 571.

[4] KNIES, D.L., GRABOWSKI, K.S., CETINA, C., "Implementing a SIMS Ion Source on the NRL Trace Element Accelerator Mass Spectrometer", Appl. Surf. Sci. 252 (2006) 7297.

[5] MAO, P.H., BURNETT, D.S., COATH, C.D., JARZEBINSKI, G., KUNIHIRO, T., MCKEEGAN, K.D., "MegaSIMS: a SIMS/AMS Hybrid for Measurement of the Sun's Oxygen Isotopic Composition" Appl. Surf. Sci. 255 (2008) 1461.

[6] SCHROEDER, J.B., HAUSER, T.M., Klody, G.M., Norton, G.A., "Initial Results with Low Energy Single Stage AMS", Radiocarbon **46** (2004) 1.

[7] WILCKEN, K.M., FREEMAN, S.P.H.T., XU, S., DOUGANS, A., "Positive Ion AMS with a Single-Stage Accelerator and an RF-Plasma Ion Source at SUERC", Nucl. Instrum. Meth. B **266** (2008) 2229.

[8] KNIES, D.L., GRABOWSKI, K.S., CETINA, C., DEMORANVILLE, L.T., DOUGHERTY, M.R., MIGNEREY, A.C., TAYLOR, C.L., "AMS Implications of Charge Changing During Acceleration", Nucl. Instrum. Meth. B **261** (2007) 582.

[9] VOCKENHUBER, C., ALFIMOV, V., CHRISTL, M., LACHNER, J., SCHULZE-KÖNIG, T., SUTER, M., SYNAL, H.-A., "The Potential of He Stripping in Heavy Ion AMS", Nucl. Instrum. Meth. B **294** (2013) 382.

Use of Micro-Raman Spectrometry for Nuclear Forensics

F. Pointurier, O. Marie

Commissariat à l'Energie Atomique et aux Energies Alternatives (CEA)
Bruyères-le-Châtel
F91297 Arpajon Cedex
France

Abstract. Thanks to its ability to carry out structural identification of small–size objects, Micro-Raman spectrometry (MRS) is a potentially interesting tool for nuclear forensics. In this communication, application of Raman spectrometry to the fast and non–destructive determination of the chemical composition of various uranium compounds will be presented and discussed. Analysis by MRS can be carried out to minute amounts of samples and to mixtures of various uranium species. Moreover, MRS can be coupled to a scanning electron microscope (SEM) thanks to a coupling device. This interface was designed to obtain topographical information (by SEM imaging), elemental composition (by EDX), and chemical information (by MRS) from the same spot without sample transfer. Different examples of analysis by MRS or SEM–MRS coupling of relevant samples for nuclear forensics will be shown.

1. Introduction

Raman spectroscopy (RS) is nowadays largely used in chemistry, biology and material science. It allows a remote, fast, very sensitive to slight structural changes, and almost non-destructive identification of chemical species and of their symmetry in a low amount of material. This technique is particularly of interest in the case of a potentially toxic or radioactive sample, of unknown origin, even of irregular shape. Moreover, several authors [1–12] demonstrated that several uranium compounds can be detected and distinguished from one another by using MRS. They also identified specific Raman bands for several uranium compounds relevant for the nuclear industry, even if most of these studies were carried out on significant amounts of materials (in the 100s of mg to the g range) as single crystals or powdered materials. However, several authors demonstrated that Micro–Raman spectrometry (MRS) is suitable for the analysis of individual microscopic objects, with a better spatial resolution (till ~1 μm) than other microanalysis techniques like micro–infrared spectroscopy (typically 20–400 μm) and micro–X-ray–fluorescence (50–3000 μm).

So, Raman spectrometry is well suited for nuclear forensics analysis, because samples are nuclear or radioactive, and non-destructive analysis must be conducted to allow applying several analytical techniques on the same sample to achieve a complete expertise. More specifically, MRS local micro–analysis capability is potentially interesting in three cases:

i) Micrometric particles are identified in the inner or outer surfaces of the container and/or packaging of the bulk seized nuclear material. These particles may be of the same composition of the bulk nuclear material (contamination) but they can also be of different composition and so bring additional information about origin of the bulk nuclear material.

ii) The seized sample is a mixture of several compounds. In such a case, a bulk analysis provides only averaged information. Micro–analysis at the scale of the single particle is therefore

necessary to identify each individual components of the mixture and to increase probabilities to identify origin of the whole sample or of its components.

iii)   The seized sample itself is a very small one, and contains only minute amounts of material. This small amount of material may have to be divided in several sub–samples for different kind of analysis, possibly carried out by different laboratories (among which destructive analytical techniques like mass spectrometry). Therefore, quantity of material in sub–samples may be too low for other structural analysis techniques.

Since 2006, CEA trace analysis laboratories in Bruyères–le–Châtel (France) are equipped with a MRS and, since 2008, with a coupling device between a SEM and the MRS. This device allows performing in–SEM Raman analysis for particles which are too small to be efficiently analyzed by MRS after location by SEM and relocation inside the MRS measurement chamber. Studies are in progress at CEA to exploit capabilities of these instruments for both safeguards and nuclear forensics [13–14]. In this paper, a few potential applications of MRS and of SEM-MRS coupling to samples deemed relevant for nuclear forensics are described and discussed.

2. Materials and instruments

2.1. Micro-Raman spectrometer

The MRS used in this study ('InVia', Renishaw, UK) is equipped with two lasers of different wavelengths: 514 nm (green) with a power of 50mW and a 785 nm (red) with a power of 300 mW. Most of the uranium compounds are colored and fluorescent, which allow choosing the laser that minimizes fluorescence for each U compound, although the 785 nm usually allows obtaining the best signal–to–noise ratios. The most appropriate substrates for both sampling particulate material and carrying out MRS analyses proved to be commercially available sticky carbon disks covered with glue (Agar, Oxford Instruments, Saclay, France). Before analyzing samples, it is necessary to calibrate the detector with respect to the wave numbers and to check the alignment of mirrors and holographic gratings. For this, a pure silicone sample is systematically analyzed to check the position (520 ± 1 cm^{-1}), resolution (<5 cm^{-1}) and intensity of the main Raman band of silicone. Laser powers are carefully optimized as lower powers do not provide enough sensitivity for micrometric targets whereas higher powers may lead to a quick thermal decomposition of the particle. Generally, powers are set to 1% of the maximal value for the 514 nm–laser (i.e. ~0.5 mW) and to 0.1% of the maximal value for the 785 nm–laser (i.e. ~0.3 mW). Analyses are generally relatively fast with typical measurement times of a few minutes. Spectral range is generally 100 cm^{-1} to 2000 cm^{-1}.

2.2. SEM

Two SEM are used to identify and locate U-bearing particles prior to the MRS analyses: a 'XL–30 ESEM' (FEI, the Netherlands) and a 'Quanta 3D FEG' (FEI, the Netherlands). Both of these instruments are equipped with an EDX analyzer and software for automated detection and location of particles (Eastern Analytical SPRL, Stevelot, Belgium). This software, called 'gunshot residue' (GSR), detects automatically particles whose average atomic number is above a given threshold (usually 20 to 25). In addition, the 'Quanta 3D FEG' is equipped with a WDX analyzer and a Focused Ion Beam (FIB) device. U-bearing particles deposited on a 1–inch diameter disk can be detected within ~8 hours. Particles as small as ~1 and ~0.5 μm are detected with respectively the 'XL 30' and 'Quanta 3D FEG' instruments. Then, the disks are transferred to the MRS.

2.3. SEM–MRS coupling

The SEM–MRS device ('SEM–SCA', Renishaw Ltd.) was designed to obtain topographical information (by SEM imaging), elemental composition (by EDX), and chemical information (by MRS) from the same spot without sample transfer. The laser beam is transferred inside the SEM measurement chamber through a mono–mode optical fiber inside a retractable arm. Raman scattering

signals are transferred to the Raman charge–coupled device (CCD) detector through the same optical fiber. The retractable arm is inserted between the BSE detector and the SEM sample holder and is positioned just ahead of the sample. The Raman scattering signal is transmitted back to the MRS following exactly the same path, through the optical fiber, and is finally directed to the CCD detector of the MRS. Particles at the disk's surface can be simultaneously viewed on the one hand with the CCD camera of the MRS thanks to a mirror attached to the retractable arm and, on the other hand, with the SE detector of the SEM. Both views are available on two separate screens. The illumination due to the laser beam can also be observed on the view provided by the CCD camera. The image of the laser beam should appear exactly in the center of the crosshairs. The spot sizes of both 514 and 785nm laser beams are less than 2 μm.

2.4. Samples

Different types of particulate materials were used for the experiments described in this paper. Small amounts of U compounds, namely U_3O_8, $UO_4 \cdot xH_2O$, UO_3, UO_2, UO_2F_2, and UF_4 produced by Areva (Pierrelatte, France), were collected with adhesive carbon disks from bulk materials (each disk containing only one compound). These materials are not reference materials, although their bulk composition is reportedly well characterized and guaranteed by the producer. Particle size distributions were large, but only particles in the size range of a few μm to a few tens of μm were studied. Raman bands regarded as the characteristic bands of a given U compound are the ones that are reproducibly observed for all particles.

Pu dioxide particles were produced by VTT Technical Research Center of Finland from certified reference material #136 solution (Pu isotopic standard, New Brunswick Laboratory, Argonne, IL, USA) using an atomizer system after chemical separation of Am [15]. The highest density of the size distribution of the particles obtained from 312 particles was in the range of 0.7−0.8 μm. The isotopic composition of Pu and U and the amount of Am were estimated by mass spectrometry techniques [15]. MRS analysis was carried out to determine the chemical form of the Pu. Particles were deposited on a glassy carbon disk. Prior to Raman analysis, 12 particles were identified as Pu–containing particles and located by SEM using EDX detector and GSR software. Sizes of these particles are typically between 1 and 2 μm.

Particles from U–Ore Concentrate (UOC) samples (commonly referred to as 'yellow cakes') of various origins were deposited by JRC/ITU (Joint European Research Center / Institute for TransUranium elements, Karlsruhe, Germany) on glassy carbon disks using the 'vacuum impactor' device specially designed by the Japan Atomic Energy Agency for this purpose. Particle size distributions are variable from one material to the other. Sizes of the analyzed particles range from 5 to 60 μm, although most of them are between 10 and 20 μm.

3. Methodologies

3.1. SEM to MRS relocation method

To relocate the particles located beforehand by SEM inside the MRS's measurement chamber, a relocation method based on the identification of landmarks on the sample holder and on suitable calculations was applied. Landmarks (see Fig. 1) are given features on two copper grids currently used in transmission electron microscopy (TEM) or –more recently– platinum crosses drawn by means of the focused ion beam device available on the 'Quanta 3D FEG' SEM. Two copper grids are glued or two crosses are engraved randomly on both extremities on the disks on which the particles are deposited. The coordinates of a particle inside the MRS are calculated using rather straightforward arithmetical operations since the positions of landmarks both inside the SEM and the MRS and the position of the particle inside the SEM with respect to the internal reference systems of each instrument are known. However, relocation methods, even with more than two marks, are not precise enough for analyzing particles smaller than ~3–4 μm because these U particles cannot be recognized (and distinguished from non–U particles) with the CCD device of the MRS. Therefore, the laser cannot be enough precisely focused on the particle.
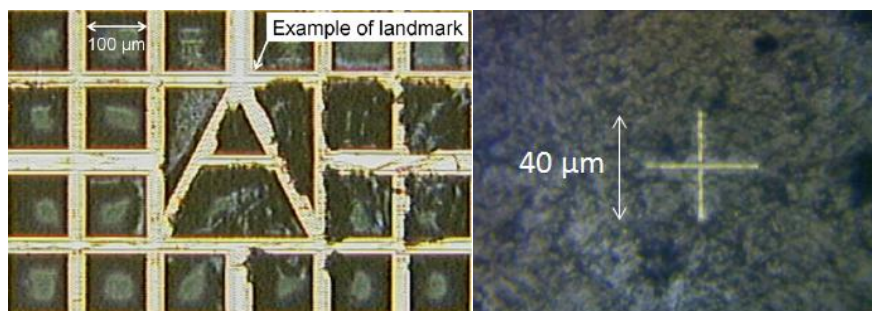
Fig. 1. Left: example of landmark chosen on TEM copper grid: the landmark is at the internal corner of the square immediately on the right above the upper extremity of the "A" letter. Right: example of cross–shaped platinum deposition used as a landmark.

3.2. In-SEM Raman analysis

As the retractable arm is inserted between the sample and the Back-Scattered Electron (BSE) detector, the latter cannot be used when the retractable arm is inserted. So, neither the BSE detector nor the GSR software can be used when the SEM–MRS coupling is active. Therefore, U particles are observed with the Secondary Electron (SE) detector. Particles at the disk's surface are simultaneously viewed on two separate screens, on the one hand with the CCD camera of the MRS thanks to a mirror attached to the retractable arm and, on the other hand, with the SE detector of the SEM. The illumination due to the laser beam is observed on the view provided by the CCD camera. To carry out a Raman analysis on μm–size particles, it is necessary to determine the position of the impact of the laser beam at the disk's surface on the SEM image with the greatest accuracy, better than a few hundredths of nanometer. However, an issue for in–SEM Raman analysis is the existing shift between the centers of the SEM and MRS images. For this, a precise landmark, clearly recognizable both with the CCD camera and with the SE detector, for instance a recognizable particle or a specific feature on a TEM grid, must be brought to the exact center of the crosshairs of the CCD image. The corresponding position of the landmark on the SEM image is therefore noted as the real position of the laser beam when focused on the disk. The shift between the centers of the CCD and SE images can be as high as 20 μm. Moreover, this shift may vary from one part of the disk to the other and must be determined frequently. It should be noted that the same magnitude ($\times500$) must be applied for both SEM (SE detector) and Raman (CCD camera) images.

It should be noted that a signal loss by a factor of ~25 is observed when performing Raman analysis on U particles using the SEM–MRS coupling with respect to the MRS alone. Although the background is also reduced by a factor of ~5, the net signal–to–noise ratio obtained with the SEM–MRS coupling is lower by roughly one order of magnitude than that of the stand-alone MRS.

Lastly, as mentioned previously, U compounds are very sensitive to high laser beam intensities. The compromise between a too low laser power (no detected signal) and a too high laser power (destruction of the particle) may be harder to obtain with SEM–MRS coupling than with the stand–alone MRS, because analyzed particles contains a very low amount of material (on the order of a few picograms for a 1 μm particle). For in–SEM Raman analysis, the powers of both lasers are attenuated thanks to attenuation filters designed to transmit 0.3%, 1%, 3%, 10%, 25%, 50%, and 100% of the incident laser light (no 1% and 3% filters are available in the case of the 514 nm–laser), respectively. However, the actual transmission of these filters can be somewhat different from the theoretical values.

4. Examples of results

4.1. Particles of various U oxides

The different U oxides used in the nuclear industry (UO_2, UO_3, U_3O_8, $UO_4 \cdot xH_2O$) cannot be reliably distinguished by SEM. Moreover, other usual analytical techniques (like XRF) require larger amounts

(milligram range) and are therefore not applicable to µm–size particles. To ensure the applicability of MRS to identify relevant U compounds contained in particles coming from 'real–life' samples, particles of each U oxide species deposited on graphite disks were analyzed by stand–alone MRS (particles from 5 µm to tens of µm) and by SEM–MRS coupling (particles as small as 2–3 µm).

The key result is that all U oxide compounds can be systematically distinguished at the particle's level, by stand–alone MRS [13]. For each U oxide, specific Raman bands were reproducibly observed, for several tens of particles of each species (see Table 1). Moreover, most of these bands match published values, even if other authors analyzed higher amounts of materials. Observed differences between observed and published data, for UO_3 and –to a lesser extent– for U_3O_8, can be explained by existence of several phases for these compounds.

However, analysis of 'real–life' samples, for which U particles of known composition are mixed with 'environmental dust' (mineral organic and particles) proves to be much more difficult. Until known, characteristic bands observed without environmental dust are not recovered when environmental dust is added. This phenomenon is currently not explained. However, this drawback is less important in the case of nuclear forensic samples (i.e. mainly made of nuclear material) than for typical safeguard samples (i.e. 'swipes') for which environmental dust is generally largely dominant.

Table 1. Main Raman bands observed for U oxides particles with the stand–alone MRS.

U compounds	Main Raman bands (cm^{-1})
UO_2	445 (s), 1150 (w)
U_3O_8	351 (m), 412 (s), 487 (m), 810 (s)
UO_3	845 (s), 1052 (w)
$UO_4 \cdot xH_2O$	823 (s), 867 (m)

s = strong intensity, m = medium intensity, w = weak intensity

When analysis is carried out by means of the SEM–MRS coupling, typical Raman bands of the studied U oxide species were also successfully observed for particles collected with sticky carbon tapes, although in–SEM Raman spectra are of poorer quality than stand–alone MRS spectra [14]. However, only UO_2 and UO_3 compounds are correctly identified for most of the particles when particles are deposited on glassy graphite disks.

Regarding the minimal size of analyzed particles using SEM–MRS coupling, Raman analyses of particles smaller ~2 µm proves to be very difficult: many attempts must be carried out before obtaining characteristic Raman bands. This size limitation is due to the extremely low amount of material available (and consequently to the very low Raman scattering obtained), to the difficulty to focus exactly the laser beam (whose diameter is larger than 1 µm) on the particle, and, lastly, to the high probability to 'burn' the particle by a too high laser emission. Nevertheless, in some cases, UO_2, UO_3, U_3O_8, and UO_4 $x(H_2O)$ particles with sizes between 1 and 2 µm were successfully analyzed. However, analysis of U particles smaller than 1 µm, which may be the physical limit for application of in–SEM Raman analysis to such small objects, was impossible [14].

4.2. *UO_2F_2 particles*

In nuclear forensic cases, one can imagine that it can be of interest to identify fluorinated U compounds in particles, either in a 'side–sample' (i.e. particles in packaging, containers, etc.) or in a mix of different compounds. SEM and SIMS [16] allows identifying compounds whose major elemental constituents are U, O and F, but not to distinguish, for instance, between UF_4 and UO_2F_2. Again, MRS analysis carried out on particles from bulk nuclear material of known stoichiometric composition (UF_4 and UO_2F_2). Characteristic reproducible Raman spectra were obtained for both of these compounds [13]. In the case of UO_2F_2, a strong intensity band, also observed [1,5,17,18] or predicted [19] by other authors, was systematically detected at 867 cm^{-1} in analyzed particles. UF_4 is reportedly very difficult to analyze by Raman spectrometry because this compound is highly fluorescent and easily degraded by laser emission. To our knowledge Krasser and Nürnberg [20] were

the only authors which successfully observed Raman bands for UF_4 thanks to a special optical arrangement of the sample to secure a tolerable noise level permitting unequivocal identifications of the Raman bands. Spectra obtained at CEA for UF_4 particles were obviously different from the ones of UO_2F_2, although Raman bands mentioned by Krasser and Nürnberg were not observed. Obtained spectra have in common a very high background and a single and very broad band whose location depends on the laser wavelength, respectively at ~300 cm^{-1} with the 785 nm–laser and at ~900 cm^{-1} with the 514 nm–laser. These broad bands are possibly composed of several bands, with close wavenumbers and relatively poor resolutions. The weak band weak band at 915 cm^{-1} previously reported by Pidduck at al. [1] and Pointurier et al. [13] for UF_4 was most probably due to anhydrous UO_2F_2 [5]. Be that as it may, MRS allows identifying and distinguishing UF_4 and UO_2F_2 at the particle's level. However, a relatively long observation of the UO_2F_2 particle by SEM should be avoided as electron beam bombardment apparently leads to a structural degradation of the particle which prevents further MRS analysis [21].

4.3.   *Pu oxide particles*

In the past decades, a few cases of seizures of small amounts of Pu nuclear material were reported. In such cases, knowledge of the chemical form of the Pu compound, in the bulk material but also at the particle's level, is very useful. Data about Raman bands of Pu oxide compounds is extremely scarce. In the present study, the produced particles were deposited on an adhesive carbon disk for SEM observation [15]. Twelve Pu particles were located by SEM equipped with EDX spectrometry. The micro-Raman analysis was performed for these 12 particles using specifically the SEM−MRS coupling. All particles had nearly spherical geometry with diameter between 1.4 and 2.4 μm. The laser used was the 514 nm one, the laser power was set to ~0.25 mW (attenuation of 0.5%) and analysis duration was 120 s. The integrated peak area was in the range of 9000−17300 counts. A single band was observed in the range of 474.9−476.4 cm^{-1} with a bandwidth in the range of 23.3−28.9 cm^{-1} [15]. This is consistent with the band observed by Begun et al. [22] at 478 cm^{-1} with a 514 nm–laser, a power of 100 mW and attributed to polycrystalline PuO_2. Therefore, the particles were identified as PuO_2. One typical example of the micro-Raman spectra measured and the corresponding electronic image are given in Fig. 2.
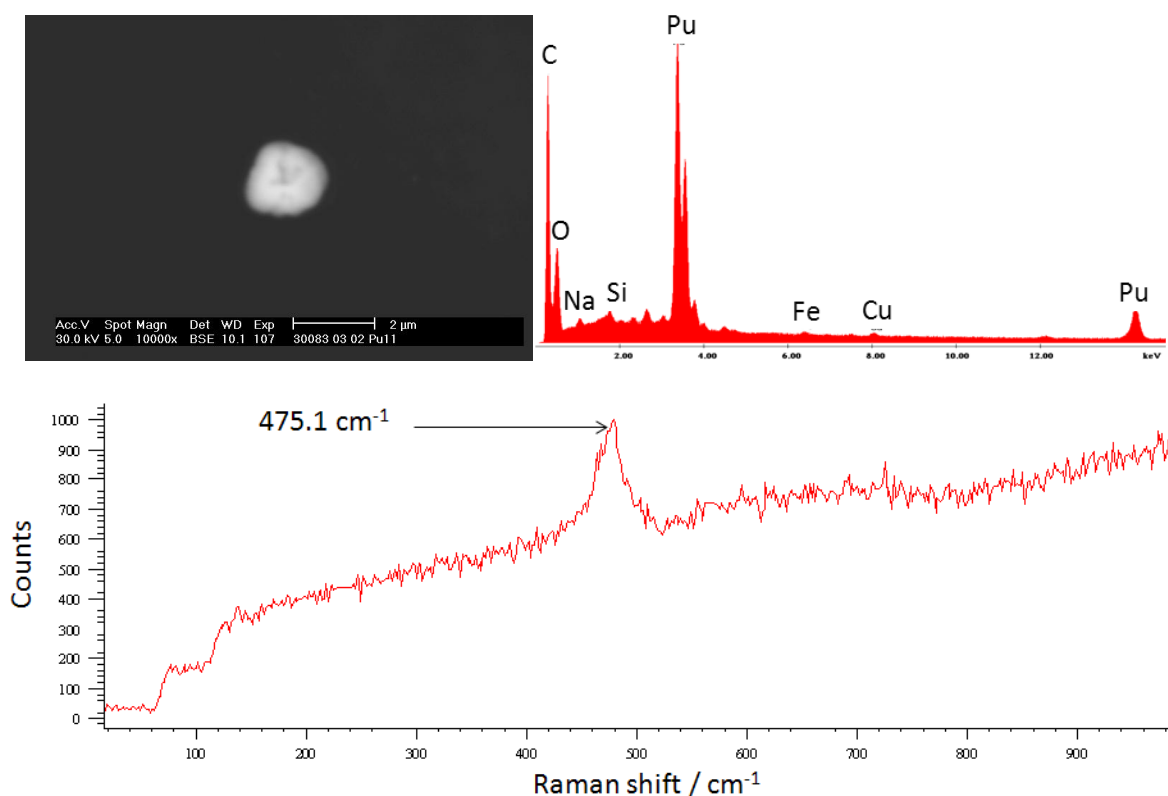
Fig. 2. Typical example of a Pu oxide particle ('particle #07') analyzed by SEM–MRS coupling: electronic image (top, left), EDX spectrum (top, right) and Raman spectrum (bottom).

4.4. *UOC particles*

In the frame of collaboration between CEA and JRC/ITU, 10 particles from 13 different UOCs of various origins were analyzed both by SEM/EDX and MRS. Data treatment (background subtraction, curve fitting, peak identification and integration, etc.) was carried out with the 'Wire 3.4' software. Particle sizes ranged from ~5 to ~60 µm. Only the 785 nm–laser was used and focused on particles with the ×50 lens. Depending on sample's band intensities and fluorescence background, laser attenuation was 0.1% or 1%, and spectrum acquisition time was 10×10 s or 10×60 s. Spectra were measured between 100 and 2000 cm^{-1}, so as to detect peaks related to the U compound itself (100–900 cm^{-1} region) and peaks related to anions (sulfates, carbonates, nitrates, etc.) present as impurities in the UOCs (900–2000 cm^{-1} region). Preliminary results are promising: Raman spectra are quite reproducible between particles from the same sample (see Fig. 3), although for some UOCs two or three types of spectra are obtained, and, most of all, typical spectra from different UOCs show significant differences. This suggests that various UOCs could be distinguished and identified based on their Raman spectra. However, more measurements must be carried out and results will be compared with the ones obtained by JRC/ITU with other types of Raman spectrometers on larger amounts of the same UOCs [23]. This work will be the subject of a future article.
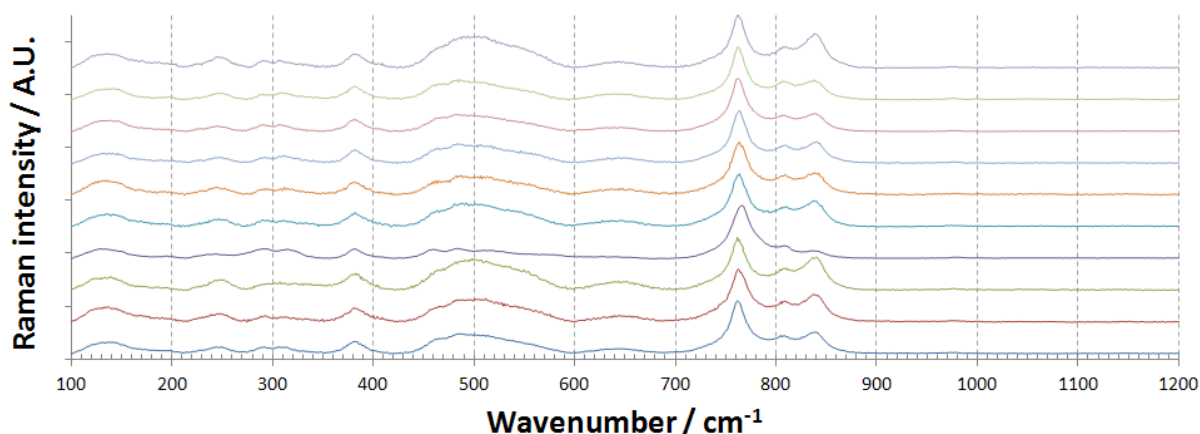

Fig. 3. Background–corrected and normalized spectra for 10 particles of the UOC 'Union Carbide'. Three main reproducible bands attributable to uranyl ion (UO_2^{2+}) stretching are observed for the 10 analyzed particles: 763±1 cm^{-1}, 809±1 cm^{-1} and 839±1 cm^{-1}.

5. Conclusions

The few examples described in this paper show that micro–Raman spectrometry is of potential interest for nuclear forensics analysis. This technique can be obviously applied to 'bulk' seized samples but, thanks to its capability to analyze micrometric objects, is also relevant in some specific cases: i) when micrometric actinide particles of interest are identified in the inner or outer surfaces of the container and/or packaging of the bulk seized nuclear material; ii) when the seized sample is a mixture of several compounds which must be identified individually by analysis at the scale of the single particle, and iii) when the seized sample contains only minute amounts of material. In such cases, the most usual U compounds in the nuclear industry, as well as Pu dioxide, can be identified in µm–size particles, provided that only limited amounts of 'environmental dust' are also present around the actinide particles. Moreover, work presently implemented both at JRC/ITU and CEA strongly suggests that Raman spectrometry analysis may provide specific signatures for UOCs, even at the particle's level.

More work has to be done notably to demonstrate feasibility of MRS analysis of U particles available in 'environmental samples', for which particles of interest are mixed with environmental dust (cellulose, iron oxides, debris of soils or biota, etc.). Besides, database for U compounds has to be enlarged to all crystalline species of UO_3 and U_3O_8 (significant differences are observed between results published by various authors for these species), and to UOCs.

REFERENCES

[1]   PIDDUCK, A.J., HOULTON, M.R., WILLIAMS, G.M., DONOHUE, D.L., A multi-technique approach to environmental particle analysis for nuclear safeguards, IAEA-CN-148/115, Proceedings of the Symposium on International Safeguards, Vienna, Austria 16–20 (October 2008) 781–789.

[2]   KIPS, R., HOULTON, M.R., LEENAERS, A., MARIE, O., PIDDUCK, A.J., POINTURIER, F., STEFANIAK, E., TAYLOR, P.D.P., VAN Den BERGUE, S., VAN ESPEN, P., WELLUM, R., The analysis of fluorine in uranium oxyfluoride particles as an indicator for particle ageing, Spectrochim. Acta Part B **64** (2009) 199–207.

[3]   MELLINI, M., RICCOBONO, F., Chemical and mineralogical transformations caused by weathering in anti-tank DU penetrators ("the silver bullets") discharged during the Kosovo war, Chemosphere **60** (2005) 1246–1252.

[4]   ALLEN, G.C., BUTLER, I.S., TUAN, N.A., Characterisation of uranium oxides by micro-Raman spectroscopy, J. Nucl. Mat. 144 (1987) 17–19. F. Pointurier, O. Marie / Spectrochimica Acta Part B **65** (2010) 797–804 803

[5]   ARMSTRONG, D.P., JARABEK, R.J., Micro-Raman spectroscopy of selected solids, W.H. Fletcher, Appl. Spectrosc. **43** (1989) 461–468.

[6]   BUTLER, I.S., ALLEN, G.C., TUAN, N.A., Micro-Raman spectrum of triuranium octoxide, U_3O_8, Appl. Spectrosc. **42** (1988) 901–902.

[7]   ROEPER, D.F., CHIDAMBARAM, D., HALADA, G.P., CLAYTON, C.R., Development of an environmentally friendly protective coating for the depleted uranium — 0.75 wt.% titanium alloy. Part IV. Vibrational spectroscopy of the coating, Electrochimica Acta **51** (2006) 4815–4820.

[8]   AMME, M., RENKER, B., SCHMID, B., FETH, M.P., BERTAGNOLLI, H., DÖBELLIN, W., Raman microspectrometric identification of corrosion products formed on UO_2 nuclear fuel during leaching experiments, J. Nucl. Mat. **306** (2002) 202–212.

[9]   MANARA, D., RENKER, B., Raman spectra of stoichiometric and hyperstoichiometric uranium dioxide, J. Nucl. Mat. **321** (2003) 233–237.

[10]   STEFANIAK, E.A., ALSECZ, A., SAJO, I.E., WOROBIEC, A., MATHÉ, Z., TÖRÖK, S., VAN GRIEKEN, R., Recognition of uranium oxides in soil particulate matter by means of µ-Raman spectrometry, J. Nucl. Mat. **381** (2008) 278–283.

[11]   PODOR, R., Raman spectra of the actinide-bearing monazites, Eur. J. Mineral. **7** (1995) 1353–1360.

[12]   GRAVES, P.R., Raman microprobe spectroscopy of uranium dioxide single crystals and ion implanted polycrystals, Appl. Spectrosc. **44** (1990) 1665–1667.

[13] POINTURIER, F., MARIE, O., Identification of the chemical forms of uranium compounds in micrometer-size particles by means of micro-Raman spectrometry and scanning electron microscope, Spectrochimica Acta Part B **65** (2010) 797–804.

[14] POINTURIER, F., MARIE, O., Use of micro-Raman spectrometry coupled with scanning electron microscopy to determine the chemical form of uranium compounds in micrometer-size particles, J. Raman Spectrosc. **44** (2013) 1753–1759.

[15] SHINONAGA, T., DONOHUE, D., AIGNER, H., BÜRGER, S., KLOSE, D., KÄRKELÄ, T., ZILLIACUS, R., AUVINEN, A., MARIE, O., POINTURIER, F., Production and Characterization of Plutonium Dioxide Particles as a Quality Control Material for Safeguards Purposes, Anal. Chem. **84** (2012) 2638−2646.

[16] FAURÉ, A.L., RODRIGUEZ, C., MARIE, O., AUPIAIS, J., POINTURIER, F., Detection of traces of fluorine in micrometer sized uranium bearing particles using SIMS, J. Anal. Atom. Spectrom. **29** (2014) 145–151.

[17] KIPS, R., PIDDUCK, A.J., HOULTON, M.R., LEENAERS, A., MACE, J.D., MARIE, O., POINTURIER, F., STEFANIAK, E.A., TAYLOR, P.D.P., VAN Den BERGHE, S., VAN ESPEN, P., VAN GRIEKEN, R., WELLUM, R., Determination of fluorine in uranium oxyfluoride particles as an indicator of particle age, Spectromchim. Acta B**64** (2009) 199–207.

[18] KIPS, R., KRISTO, M., HUTCHEON, I., Progress report March–October 2009, Study of Chemical Changes in Uranium Oxyfluoride Particles, Progress Report, LLNL–TR–420742 (November, 25, 2009).

[19] OHWADA, K., Uranium–fluorine lattice vibration of uranyl fluoride, J. Inorg. Nucl. Chem., **33** (1971) 1615–1623.

[20] KRASSER, W., NÜRNBERG, H.W., Vibrational spectra and force constants of uranium tetrafluoride, Spectrochim. Acta **62A** (1970) 1059−1062.

[21] STEFANIAK, E.A., POINTURIER, F., MARIE, O., TRUYENS, J., AREGBE, Y., In-SEM Raman microspectroscopy coupled with EDX – a case study of uranium reference particles, Analyst **139** (2014) 668–675.

[22] BEGUN, G. M., HAIRE, R. G., WILMARTH, W. R., PETERSON, J. R. J., Raman spectra of some actinide dioxides and of EuF_2, Less-Common Met. **162** (1990) 129−133.

[23] HO MER LIN, D., MANARA, D., VARGA, Z., BERLIZOV, A., FANGHÄNEL, T., MAYER, K., Applicability of Raman spectroscopy as a tool in nuclear forensics for analysis of uranium ore concentrates, Radiochim. Acta **101** (2013) 779–784.

Forensic and Medical Aspects of Radiation Accidents Investigation

K.V. Kotenko, Yu.E. Kvacheva, E.O. Granovskaya, B.A. Kukhta

State Research Center – Burnasyan Federal Medical Biophysical Center of Federal
Medical Biological Agency,
Moscow, Russian Federation

Abstract. Practical experience of radiation emergency response [1] can be used in the investigation of cases involving unauthorized use of ionizing radiation sources. Investigation of radiation accidents with fatal and non-fatal lesions sometimes is very difficult. Results of biomedical and instrumental analyses, carried out after the emergency medical activities, are important and sometimes crucial to establish details of the accident. Based on them, the experts can substantially assist in the investigation: help to formulate possible versions of an incident and determine further investigative leads. The following aspects should be taken into account within such biomedical analyses.

1. Internal Exposure

Based on the experience, summarized in a number of special publications [2-6], the following radionuclides, widely used in industry and medicine (or resulting from the operation of ionizing radiation sources), are generally accepted to be radiologically dangerous: ^{3}H, ^{241}Am, ^{137}Cs, ^{60}Co, ^{131}I, ^{210}Po, ^{238,239}Pu, ^{252}Cf, ^{192}Ir, ^{235}U, ^{226}Ra, ^{89,90}Sr, ^{144}Ce. These radionuclides are alpha and beta emitters (except for cobalt, and cesium, which are gamma-emitters). So, they may cause radiation damage primarily in case of intake into the body. There are several routes of intake of radionuclides: inhalation (with inhaled air), ingestion (with food and water), through intact or burned skin or wounds. The main routes of intake, transfer and excretion are shown in Fig. 1.
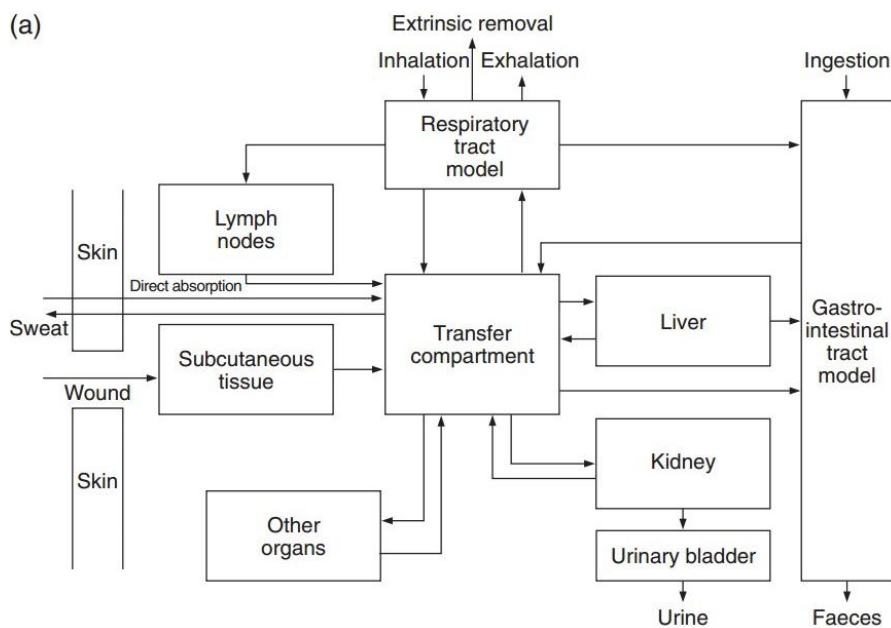

FIG. 1 The main routes of intake, transfer and excretion of radioactive substances [7].

In case of inhalation of radioisotopes the degree and nature of lesions of respiratory organs depend primarily on absorbability of them across the air-blood barrier after deposition on the surface of respiratory tract. It is directly related to the type of an incorporated radioactive chemical compound. There are three types of chemical compounds in terms of rate of transition of the deposited radioactive material into the internal environment of the body: F - fast, M - medium, S - slow [8]. Hardly soluble radioactive substances or their compounds are partly removed from the airways with mucus due to work of the ciliated epithelium. The rest is retained in the lung tissue and has mainly local effect, which can lead to development of deterministic or stochastic effects of varying severity.

In case of contact with intact skin radioactive substances cause local injuries. The rate of their development and severity depend on the absorbed dose and the rate of absorption of the radioactive material.

In cases of intake of radioactive substances through the gastrointestinal tract the following facts must be considered. Substances with low absorption ability (less than 5%) have mainly local effect. Well-absorbed radioisotopes (15-20%) are transferred into the blood and then uniformly distributed throughout the body or selectively concentrated in organs and tissues of main deposition (organotropic) [9-11]. ^{137}Cs, ^{3}H and ^{210}Po are usually uniformly distributed throughout the body. ^{238,239}Pu, ^{241}Am, ^{89,90}Sr, ^{235,234,238}U, ^{224,226}Ra, ^{131}I are organotropic radionuclides. The organotropic radionuclides can be divided into the following groups: (1) osteotropic, (2) mainly deposited in liver and bones. A number of radioisotopes with low absorption ability can cause ulcero-necrotic changes in the gastrointestinal tract in case of ingestion.

In particular, ^{144}Ce oftener affects distal small intestine, ^{241}Am - duodenum and small intestine, ^{239}Pu - colon. Also, keep in mind that there is no system failure of blood and gonads in cases of ingestion intake of radionuclides not combined with external irradiation.

When transferred into the blood through skin, lungs or intestines radioactive substances selectively concentrate in organs of main deposition. So, the signs of internal radiation lesions due to accumulation can be observed in clinical and pathological-anatomical characteristics of radiation sickness caused mainly by internal exposure.

In particular, 90% of the radioactive strontium is deposited in bones, predominantly in metaphyses of long bones and a spongy layer of trabecular bones (e.g. in sternum), causing even in the early days deep distortion and suppression of normal physiological bone formation, which does not occur in case of acute radiation disease due to external exposure.

^{131}I is rapidly accumulated in the thyroid regardless of intake pathway. One can observe extensive hemorrhages in soft tissues of neck and in thyroid, destructive changes up to focal or total necrosis of thyroid parenchyma (bleedings occurring at the beginning of radiation disease are usually mild).

In case of intake of transuranic elements (Pu and Am) up to 90% of the total activity transferred into blood is deposited in liver, and to a lesser extent in kidney. ^{137}Cs is predominantly deposited in heart muscle. So, lesions of mentioned organs can be observed at autopsy.

If intake of radioactive substances is suspected (or there is reliable information), it is important to confirm this information using *in vivo* or *in vitro* analyses in order to determine pattern of distribution of radionuclides through tissues and organs of the body and level of their radioactivity.

In order to assess intake of radioactive material and internal dose it is necessary to have the following:

(1) Metrologically certified procedures of radiochemical analysis, including the analyses selective to the required radionuclides;
(2) Accepted measuring instruments, including whole body counters, radiometers and spectrometers;
(3) Verified computational techniques, including the techniques using the Monte Carlo method;

(4) Specialized software that allows you to assess the intake and doses. In addition, the specialists should have the research protocols approved by the relevant authorities. Sampling and subsequent analysis according should be carried out in accordance with such protocols.

In cases of suspected intake of gamma emitters first of all a survey using whole body counter should be carried out (*in vivo* analyses). If intake of beta-or alpha-emitters is suspected biophysical studies come to the fore (*in vitro* analyses using the appropriate equipment: radiometers for measuring of total alpha and beta activity, alpha- and beta- spectrometers, LS (liquid scintillator) spectrometers, mass spectrometers). The procedure of sampling is very important for biophysical analyses. Sampling of organs must be performed in accordance with the anatomical standard: pieces of organs and tissues (weight not less than 30-50 g) should be taken with clean tools and put in chemically clean vessels without using fixative, the vessels should be tightly closed and sealed. The analysis of biological secretions: nasal swabs, samples of feces and urine, for the content of radioactive substances is of particular importance while patient examination. Biophysical analysis of urine and feces is efficient in terms of assessing the levels of intake and retention. Excretion of radionuclides with urine or feces is irregular. So, the daily amount of excreta for several consecutive days should be collected. Use clean, tightly sealed containers.

Intake and internal dose can be assessed on the basis of the measured levels of excretion and retention using the published models of biokinetics of radionuclides, similar to the one shown in Fig. 1. Moreover, in some cases, certain assumptions about the nature of a radioactive substance and timing of intake can be made.

2. External exposure

In case of external exposure, different conditions of irradiation have different effects on clinical and anatomical characteristics of radiation injury. This is due either to a different degree of severity of pathoanatomical changes or specific localization of the most pronounced effects, or various sequels of the prior disease (e.g., infection).

It is important to consider qualitative and quantitative characteristics of pathological processes in order to help assessing the morphophysiological picture. It is necessary to assess the full range of different conditions, which could cause the main damage.

In emergency situations absorbed dose of ionizing radiation for each case of radiation injury sometimes is not known. At the same time, such information is necessary. Instrumental (eg, EPR spectrometry, phantom modeling) and medical and biological methods can be used to get such estimates In fatal case, if no measurements or estimates of levels of external doses are available, pathologist or forensic expert performing autopsy of a person died from radiation sickness (or if radiation sickness suspected) should try to estimate absorbed dose on the basis of pathoanatomical changes.

To date a number of methods of biological dosimetry, which allow rather accurate assessing of total and local absorbed doses on the basis of early reactions of an irradiated person, have been developed. Objective criteria such as rate of development, type and extent of chromosomal damages in red blood cells, skin reaction (primarily its severity on different areas of skin should be estimated) are used for this purpose.

There are unlimited variants of non-uniform exposure with a primary direct effect of ionizing radiation on a particular part of the body. So, it is important to identify the basic scenarios where the absorbed dose to head, chest, abdomen or limbs is maximal:

— In cases of non-uniform external radiation exposure a pathologist should take into account that an isolated or predominant exposure of head to large dose leads to lesion of its skin, mucous membranes of mouth and nose, eyes and brain;

— Irradiation of chest results in lesion of lungs, heart muscle, spine (with peripheral spinal disorders), bone marrow of sternum and vertebras;
— Irradiation of abdomen and pelvis results in lesions of small intestine up to development of ulcero-necrotic changes and peritonitis. Sometimes it may result in lesion of colon and other internal organs, e.g. kidneys;
— Irradiation of limbs results in lesions of skin and skeletal muscles.

Macroscopic and especially microscopic examination of hemopoietic organs of a deceased is of particular importance in order to establish presence / absence of significant differences in condition of bone marrow, taken from different parts of the body, as well as the discrepancy between severity of suppression of hematopoiesis and characteristics of peripheral blood.

An example of non-uniform gamma exposure resulted in a massive heavy lesion of intestine (120-160 Gy), spine (50 Gy) and lumbar spine is the case of radiation injure described by N.A.Kraevskiy, 1962 [12]. Aplastic anemia in vertebral bone marrow combined with normal content of hematopoietic parenchyma of other skeleton sites was observed.

The period of time passed after radiation injury can be assessed on the basis of morphological characteristics of bone marrow. Under doses at which the hematopoietic form of radiation sickness takes place, the elements of stroma and plasma cells dominate in cellular composition in the first 2-3 weeks of the disease. Later, after 4 weeks, granular lymphocytes appear. Then morphological signs of early recovery can be observed: the number of hematopoietic stem cells and mitosis increase [13].

Using modern immunomorphological methods of staining of bone marrow sections an expert can make a rough estimation of radiation injury severity. Under the doses within "marrow failure" range (1-10 Gy) the number of dying cells is low - an average of 4-5 in a field of view of a microscope. Under higher doses (intestinal and cerebral form of radiation sickness) - cell death exceeds 50% [14].

3. Conclusion

Thus, a lot of questions traditionally asked experts by investigating authorities can be answered on the basis of the assessment of nature and severity of lesions observed on corpse or body of survivor. They are the following:

— Diagnostics of radiation injures and making decision on possibility or impossibility of development of such lesions under conditions specified in a case files;
— Determination of period of time passed after radiation accident and mechanism of radiation injury development in order to reconstruct circumstances of a case;
— Assessment of exposure conditions, intake of radioactive material, levels and rates of external and internal doses, etc.

Within the investigation of radiation accidents biomedical analyses are necessary. They should be performed to ensure objectivity and scientific relevance of expert's conclusions.

REFERENCES

[1] ALEKSAKHIN R.M., BULDAKOV L.A., GUBANOV V.A. et al. "Radiation accidents" Edited by Ilyin L.A., Gubanov V.A. IzdAt Publisher, Moscow, 2001 (in Russian).

[2] INTERNATION ATOMIC ENERGY AGENCY, Code of Conduct on the Safety and Security of Radioactive Sources, GOV/2003/49-GC(47)/9 Annex 1, IAEA, Vienna, (2003).

[3] INTERNATIONAL ATOMIC ENERGY AGENCY, Strengthening control over radioactive sources in authorized use and regaining control over orphan sources – National strategies, IAEA-TECDOC-1388, IAEA, Vienna, (2004).

[4] Countering Nuclear and Radiological Terrorism / Ed. by S. Apikyan, D. Diamond. - Springer, 2006.

[5] SHIN H., KIM J. Development of realistic RDD scenarios and their radiological consequence analyses / Applied Radiation and Isotopes 67 (2009) 1516–1520.

[6] KUTKOV V., BUGLOVA E., MCKENNA T. Severe deterministic effects of external exposure and intake of radioactive material: basis for emergency response criteria / J Radiol Prot. 2011 Jun; 31(2): 237-53.

[7] INTERNATIONAL ATOMIC ENERGY AGENCY, Assessment of Occupational Exposure Due to Intakes of Radionuclides. Safety Standards Series No. RS-G-1.2. IAEA, Vienna, (1999)

[8] Human Respiratory Tract Model for Radiological Protection. ICRP Publication 66. Ann. ICRP 24 (1-3), 1994.

[9] MOSKALEV YU.I. Radiobiology of incorporated radionuclides. Energoatomizdat Publisher, Moscow, 1989 (in Russian).

[10] ZHURAVLEV V.Ph. Toxicology of radioactive substances. Energoatomizdat Publisher, Moscow, 1990 (in Russian).

[11] KALISTRATOVA V.S., BELYAEV I.K., ZHOROVA E.S., NISIMOV P.G., PARFENOVA I.M., TISHCHENKO G.S., TSAPKOV M.M. " Radiobiology of incorporated radionuclides." Edited by Kalistratova V.S. Publisher Burnasyan FMBC of the FMBA of Russia, 2012 - 464 p.

[12] KRAEVSKY N.A. Anatomicopathological data. In book: A case of acute radiation sickness in humans. Edited by prof. Kurshkova N.A. Medgiz Publisher, 1962. pp. 91-136 (in Russian).

[13] KVACHEVA YU.E. Human Bone Marrow Repair Processes and Cell Populations in Acute Radiation Injury: a Morphological Study // Radiation Biology. Radioecology, 2000, 40, 1: 5-9.

[14] KVACHEVA YU.E. Morphology of Radiation-induced Cell Death Types in Hematopoietic Tissue, Its Biological Essence and Significance Within the Different Stages of Acute Radiation Injury // Radiation Biology. Radioecology, 2002, 42, 5: 287-292.

BIBLIOGRAPHY

ILYIN L.A., NORETZ T.A., SCHVYDKO N.S., IVANOV E.V. Radioactive substances and skin (metabolism and decontamination). Edited by Ilyin L.A. Atomizdat Publisher, Moscow, 1972, 301 pp. (in Russian).
ILYIN L.A., IVANNIKOV A.T. Radioactive substances and wounds: metabolism and decorporation. Atomizdat Publisher, Moscow, 1979, 256 p. (in Russian).
ILYIN L.A. Radiation Medicine Guidance for Medical Researchers and Health Management Vol 2 Radiation Damage of Humans ed A Yu Bushmanov et al. Moscow: AT, ISBN 5-86656-114-X, 2001 (in Russian).

OSANOV D.P. Dosimetry and radiation biophysics of the skin. Energoatomizdat Publisher, Moscow, 1990 (in Russian).